http://ansinet.com/itj



ISSN 1812-5638

# INFORMATION TECHNOLOGY JOURNAL



Asian Network for Scientific Information 308 Lasani Town, Sargodha Road, Faisalabad - Pakistan

## Study on Air Flow Distribution of Ventilating System in the Low Pressure Chamber for Controlling the Tobacco Smoke

<sup>1</sup>Zhang Qing, <sup>2</sup>Yang Lei, <sup>1</sup>Zhao Hang, <sup>1</sup>Miao Qian, <sup>1</sup>Yang Rongchao, <sup>1</sup>Ma Ming and <sup>2</sup>Dong Fuwen <sup>1</sup>China Tobacco Standardization Research Centre, Zhengzhou, 450000, China <sup>2</sup>Zhongyuan University of Technology, Zhengzhou, 450007, China

**Abstract:** Most modern tobacco industries have chambers to evaluate the quality of tobacco samples. In the academe, this chamber should also produce a low pressure likely to the atmospheric pressure in high altitude area. A ventilation system should be used in the chamber to controlling the tobacco smoke. This study aims at the air flow distribution of a ventilation system of the chamber with the low pressure and assessing its controlling effect on tobacco smoke. Computational Fluid Dynamic method is applied for the simulation of air flow field and smoke moving path in a condition of low pressure in the chamber. Furthermore, a distance-data acquisition system is set up in the camber to monitor the air velocities of six particular positions close to inlets or outlets. The numerical simulating results in this study can show us the effect of the air flow distribution and air flow velocity in the chamber, which can be proved validity by the results from the distance-data acquisition system. In this case, the locations of the inlets and outlets of ventilation system may be the key factor in the design of the ventilation system. It can be also concluded that the better air flow distribution may decrease the turbulent circuit and reduce the dust deposit in the corners of the chamber.

Key words: Tobacco smoke, air flow distribution, chamber, low pressure, computational fluid dynamic method

#### INTRODUCTION

Recently, many modern tobacco industries have set up chambers to evaluate the quality of tobacco samples, which have low pressure conditions by simulating diverse low atmospheric pressure of cities in China. Cigarette smoke includes particular matter and CO et al. (WHO, 2008; U.S. DHHS, 2006). Without the understanding of air flow characteristics in the chamber with low pressure, tobacco smoke can never be fully controlled (Bauman and Arens, 1988; Fish et al., 1991). In this study, Computational Fluid Dynamic (CFD) method is applied for the simulation of air flow field and smoke moving path.

### MATERIAL AND METHOD

**Chamber:** A chamber in a city of central China is chosen as the test case and its schematic figure are shown in Fig. 1. The chamber is 2.1 m high and 3.3 m length and 3.0 m width. The chamber is equipped with the windtight envelope. Two inlets are set on the top of the chamber and four outlets are installed on the bottom of the chamber, which are shown in Fig. 1. The chamber works on the condition of 96000 Pa, which is same as the low

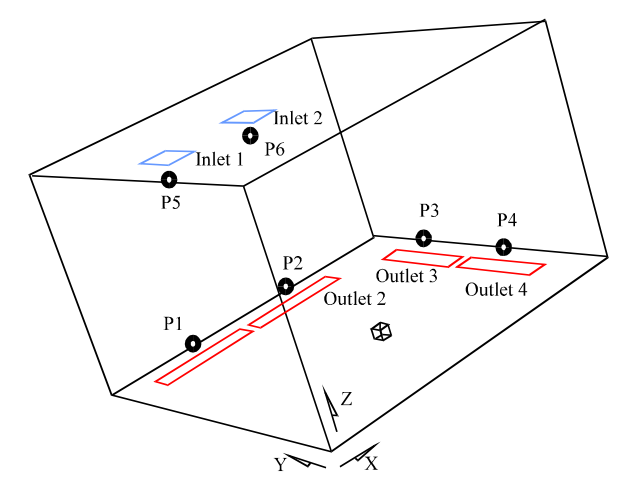


Fig. 1: Schematic of the chamber and the location of its inlets and outlets and test positions for velocity

atmospheric pressure of Xi'an city in China. In chamber, the air temperature was 22-25 degree Celsius and the relative humidity was 35-50%.

For analyzing the effect on controlling smoke by the air flow, the study has simulated the air flow distribution and velocity of five virtual vertical sections along the x-axis and four virtual vertical sections along the y-axis.

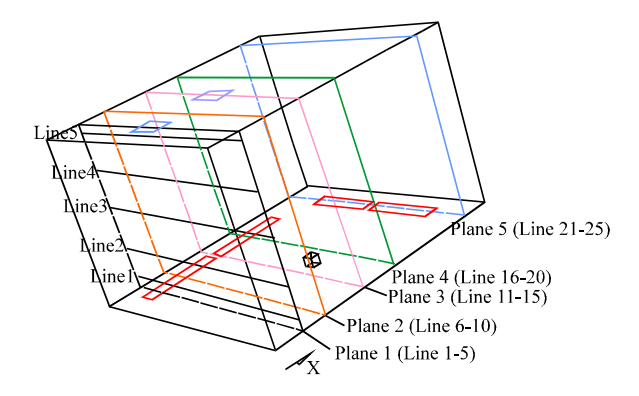


Fig. 2: Sequence and locations of the planes and lines along the x-axis

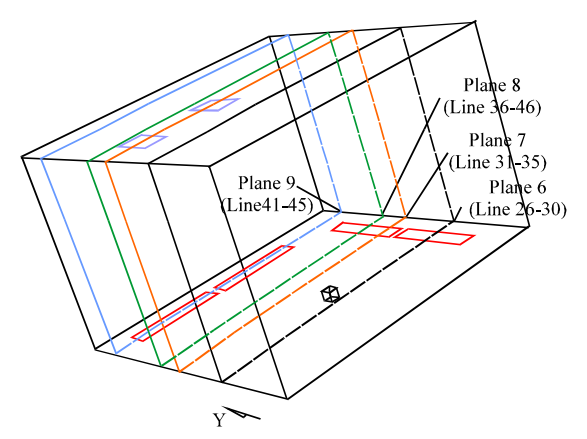


Fig. 3: Sequence and locations of the planes and lines along the y-axis

Each plane has five virtual horizontal lines along the z-axis and the total number of lines on those planes is forty five. The sequence and locations of the planes and lines are shown in the Fig. 2-3 and Table 1.

**CFD method:** Computational Fluid Dynamic method (CFD) is utilized to model the air flow distribution in the chamber. The basic conservation equation of CFD can be shown as Eq. 1:

$$\begin{split} &\frac{\partial \left(\rho T\right)}{\partial t} + \frac{\partial \left(\rho u T\right)}{\partial x} + \frac{\partial \left(\rho v T\right)}{\partial y} + \frac{\partial \left(\rho w T\right)}{\partial z} \\ &= \frac{\partial}{\partial x} \left(\Gamma \frac{\partial T}{\partial x}\right) + \frac{\partial}{\partial y} \left(\Gamma \frac{\partial T}{\partial y}\right) + \frac{\partial}{\partial z} \left(\Gamma \frac{\partial T}{\partial z}\right) + So \end{split} \tag{1}$$

Mass conservation form and momentum conservation form of Eq. 1 are the control equations for the CFD simulation of the dynamics fields on the assumption that there is no energy impact. For convenience, it is also assumed that the leakage through the gaps of the door be zero. A commercial CFD software

Table 1: Sequence of the planes and lines and their position

	Location on	Location on	Location of lines	
Plane sequence	x-axis (m)	y-axis (m)	on z-axis (m)	
Plane 1	0.43		Line1-5	
Plane 2	0.8		Line6-10	
Plane 3	1.28		Line11-15	
Plane 4	1.9		Line16-20 $z = 0.1$	0
Plane 5	2.8		Line21-25 $z = 0.5$	0
Plane 6		0.5	Line 26-30 $z = 1.0$	0
Plane 7		1.5	Line $31-35$ $z = 1.5$	0
Plane 8		1.9	Line 36-40 $z = 2.0$	0
Plane 9		2.65	Line41-45	

is used as the computational fluid dynamic tool for simulating the temperature field and velocity field before renovation and after renovation. RNG k-å model is applied in the research and the boundary conditions have two velocity inlets and four velocity outlets. The inlets of fresh air are designed as velocity inlets and outlets of exhaust air are adopted as outflow. The wall of the chamber is assumed adiabatic.

CFD simulation process: The first step is to identify a chamber that can be reproduced as a 3-dimensional CAD Solid Works engineering drawing package. The next stage is to import the files into the CFD Code preprocessor ready for solving the flow equations. Here, the flow fields boundary condition are set. These may include inlet air flow velocity, outlet air flow velocity, outlet pressure or fluid properties. The next step is to set the simulation process as a 3-dimensional, steady and laminar problem. The final step is to analyze the output data and present them in the form of velocity vector distribution and contour plots.

**Distance-data acquisition system:** A Distance-data Acquisition System (DDAS) with six test detectors is used in the chamber to prove validity of CFD results. The detectors can be rotated a few degrees for facing the max velocity direction. As shown in Fig. 1 and Table 2, four of the detectors, named as P1-P4, are located over the outlets with a height of 0.50 m and the other detectors, named as P5 and P6, are fixed just below the inlets with 0.10 m distance. The distance-data acquisition system can collect the velocities of six points simultaneously.

#### RESULTS

Operation parameter of the ventilating system: The actual ventilating rate of the tested chamber has been measured by the pitometer in a low atmospheric pressure of 96000 Pa. The air flow velocity of the inlets can be calculated by the ventilating air volume and the area of the opening of inlets. In this study, the air flow velocity of the inlets is 1.00 m sec<sup>-1</sup>.

Table 2: Six detectors and their position in the chamber

		Corresp-onding inlet or outlet	Location of test position		
Dete-ctors	Test position		Distance between the detector and the corresponding inlet or outlet(m)	Their location on x-axis, y-axis and z-axis (m)	
No.1	P1	Outlet 1	0.10	x = 0.80	
				y = 2.65	
				z = 0.10	
No.2	P2	Outlet 2	0.10	x = 1.90	
				y = 2.65	
				z = 0.10	
No.3	P3	Outlet 3	0.10	x = 2.80	
				y = 1.90	
				z = 0.10	
No.4	P4	Outlet 4	0.10	x = 2.80	
				y = 0.50	
				z = 0.10	
No.5	P5	Inlet 1	0.10	x = 0.43	
				y = 1.50	
				z = 2.00	
No.6	P6	Inlet 2	0.10	x = 1.28	
				y = 1.50	
				z = 2.00	

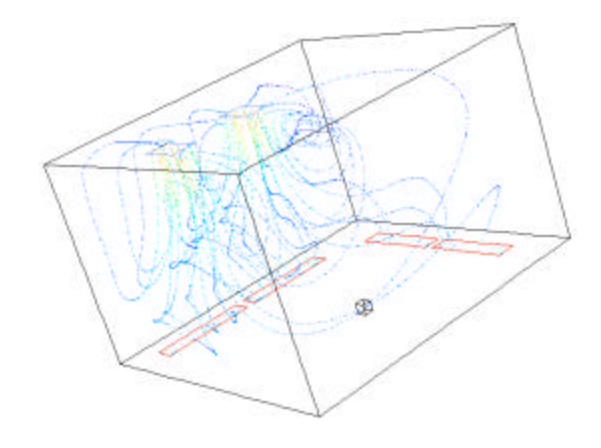


Fig. 4: Air flow tracks in the low pressure chamber

**Results of CFD:** CFD software can simulate the air flow field in the low pressure chamber on base of the designed boundary conditions. Figure 4 is the air flow tracks in the chamber with four outlets on the bottom and two inlets on the top.

Figure 5 shows the contours of velocity magnitude of the virtual planes (No. 1-5) alone x-axis.

Figure 6 illustrates the contours of velocity magnitude of the virtual planes (No. 6-9) alone y-axis:

- Velocity distribution of virtual horizontal lines (No. 1-5) on No. 1 Plane can be illustrated in Fig. 7
- Velocity distribution of virtual horizontal lines (No. 6-10) on No. 2 Plane can be illustrated in Fig. 8
- Velocity distribution of virtual horizontal lines (No. 11-15) on No. 3 Plane can be illustrated in Fig. 9

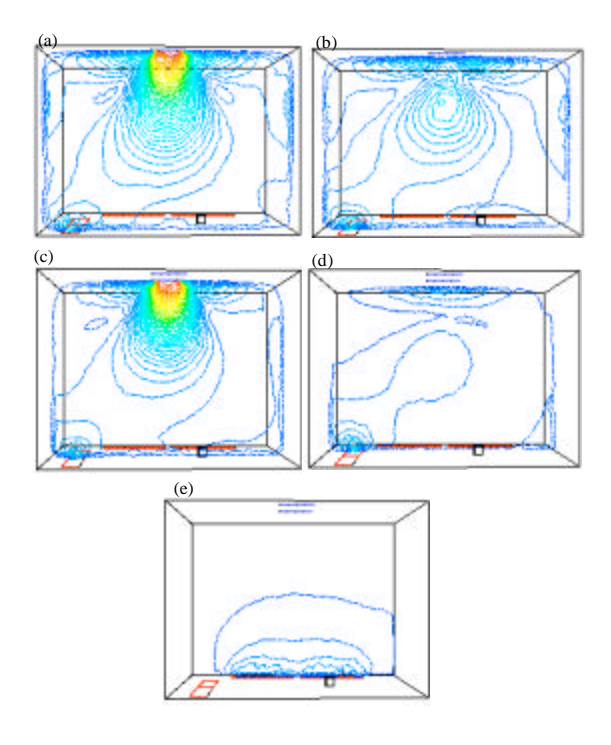


Fig. 5(a-e): Contours of velocity magnitude of No. 1
Plane to No. 5 Plane (views along positive x-axis)

- Velocity distribution of virtual horizontal lines (No. 16-20) on No. 4 Plane can be illustrated in Fig. 10
- Velocity distribution of virtual horizontal lines (No. 21-25) on No. 5 Plane can be illustrated in Fig. 11
- Velocity distribution of virtual horizontal lines (No. 26-30) on No. 6 Plane can be illustrated in Fig. 12

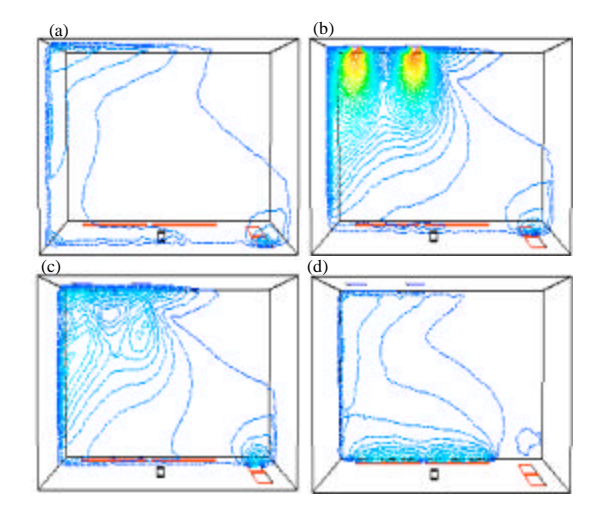


Fig. 6: Contours of velocity magnitude of No. 6 Plane to No. 9 Plane (views along positive y-axis)

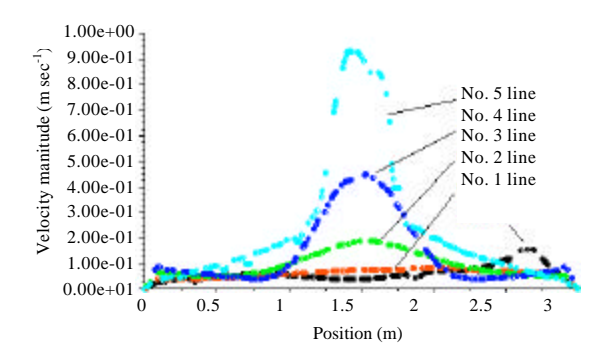


Fig. 7: Velocity distribution of horizontal lines on No. 1 Plane (views along positive y-axis)

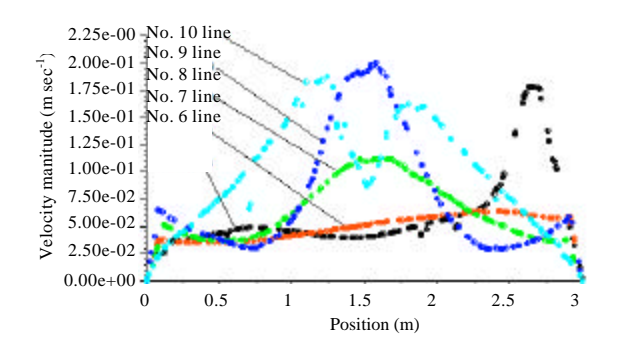


Fig. 8: Velocity distribution of horizontal lines on No. 2 Plane (views along positive y-axis)b

 Velocity distribution of virtual horizontal lines (No. 31-35) on No. 7 Plane can be illustrated in Fig. 13

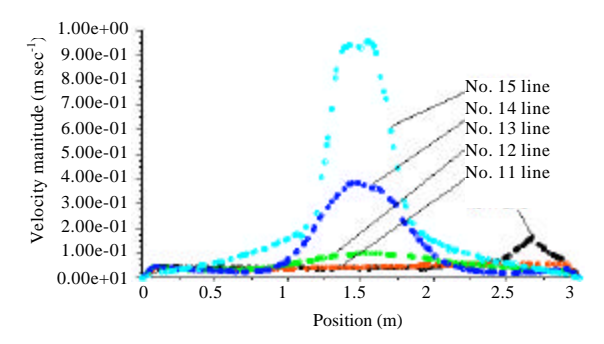


Fig. 9: Velocity distribution of horizontal lines on No. 3 Plane (views along positive y-axis)

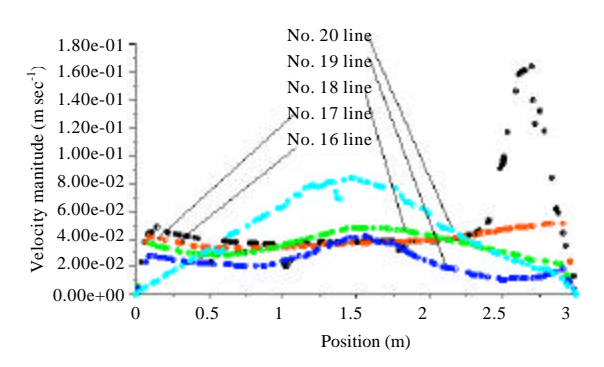


Fig. 10: Velocity distribution of horizontal lines on No. 4 Plane (views along positive y-axis)

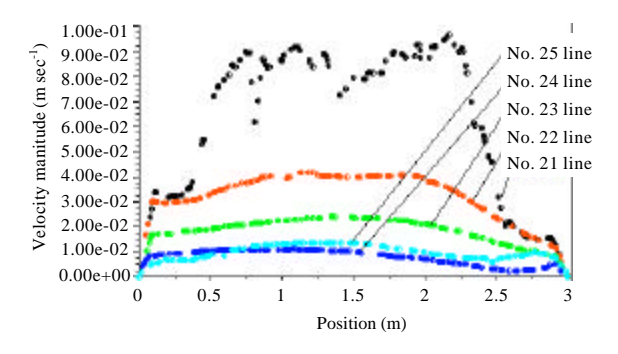


Fig. 11: Velocity distribution of horizontal lines on No. 5 Plane (views along positive y-axis

- Velocity distribution of virtual horizontal lines (No. 36-40) on No. 8 Plane can be illustrated in Fig. 14
- Velocity distribution of virtual horizontal lines (No. 41-45) on No. 9 Plane can be illustrated in Fig. 15

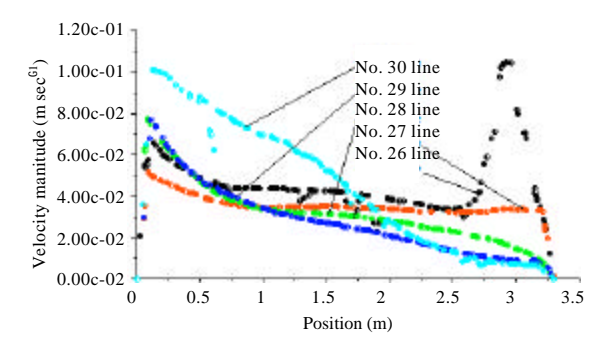


Fig. 12: Velocity distribution of horizontal lines on No. 6 Plane (views along positive x-axis)

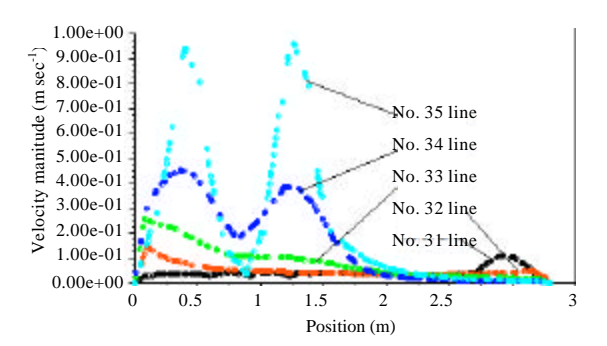


Fig. 13: Velocity distribution of horizontal lines on No7 Plane (views along positive x-axis)

Velocities collected by DDAS: The velocities in the test positions of the chamber can be collected by six test detectors of DDAS. Table 3 shows the average velocity in every test position. Minimum velocities and maximum velocities in the test positions are also listed in Tab.3 for further analysis on air flow distribution of ventilating system of the chamber.

#### DISCUSSIONS

Air flow field: The computed results of the air flow field can show that irregularly distributed outlets on the bottom and inlets on the top can make the air flow direction turbulence in the chamber. In Figure 4, there are several eddies and many curved air flow lines in the air flow field.

In Fig. 5, the contours of velocity magnitude of the virtual planes (No. 1-5) alone x-axis are different from each other. The inlets are close to two of the outlets, so that the contours between them are concentrated. On the other

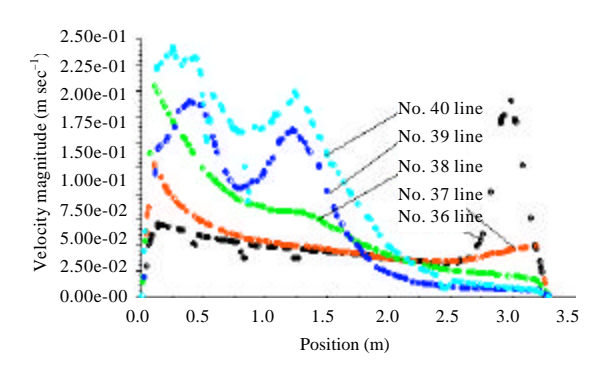


Fig. 14: Velocity distribution of horizontal lines on No. 8 Plane (views along positive x-axis)

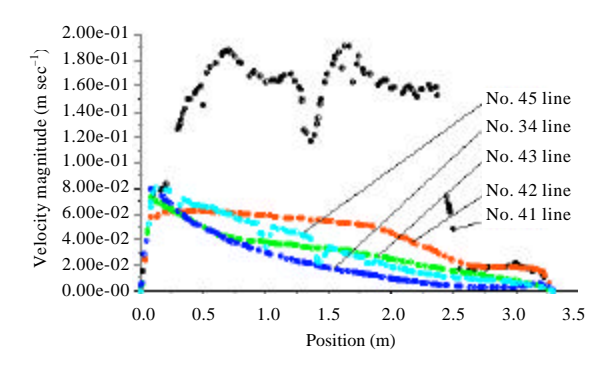


Fig. 15: Velocity distribution of horizontal lines on No. 9 Plane (views along positive x-axis)

Table 3: Velocities of the six test position in the chamber						
	Average velocity	Minimum velocity	Maximum velocity			
Test position	(m sec <sup>-1</sup> )	$(m sec^{-1})$	(m sec <sup>-1</sup> )			
P1	0.13	0.12	0.17			
P2	0.12	0.11	0.16			
P3	0.07	0.05	0.11			
P4	0.06	0.05	0.10			
P5	0.60	0.67	0.92			
P6	0.67	0.62	0.95			

hand, the rest contours in No. 4 and 5 are scattered. This can be proved by the results in Fig. 6, which has a sparse distribution as to the contours of velocity magnitude of the No. 6 virtual planes. This is in agree with the results in the previous study (Panagopoulos *et al.*, 2011).

**Velocity distribution:** Figure 7 shows the velocity distributions of virtual horizontal lines (No. 1-5) on No. 1 Plane. Obviously, the high velocity of air flow, which belongs to the results of No. 5 Line, is about 0.93 m sec<sup>-1</sup>. This velocity point is located in the position of 0.43 m on the positive x-axis, 1.50 m on the positive y-axis and 2.00 m on the positive z-axis. This explains that the inlets

affected the velocity distributions. Fig. 8-9, Fig. 13-14 can also demonstrate this option.

Fig. 10 illustrates the velocity distributions of virtual horizontal lines (No. 16-20) on No. 4 Plane. Although the max velocity of No. 16 Line is higher than those of other lines, the highest velocity about 0.17 m sec<sup>-1</sup> on No. 16 Line shows that the outlet can not work efficiently. Figure 12 and Fig. 15 can also support this view. However, the max velocity of No. 21 Line in Fig. 11 is about 0.95 m sec<sup>-1</sup>, which shows a strange result that the most venting volume is concentrated to be exhausted by the outlets far away the inlets.

**Venting volume:** The virtual exhaust volume for the chamber with low pressure is 720 m<sup>3</sup> h<sup>-1</sup>. In another word, the ventilation rate for the chamber is about 35 times. This value can meet the requirement of the admitted low ventilation rate in the Chinese standard, which is designed as about 12 times (CNIS GBZ1, 2010).

#### Comparisons of the results from DDAS and CFD:

Table 3 demonstrates that DDAS results for the velocity in the four test positions, which are P1, P2, P3 and P4, agree with CFD results. However this is not true for the velocities in P5 and P6, where there are 40%-60% gaps between the results collected by DDAS and CFD methodology. The grille diffuser may contribute to those gaps because the high velocities from the inlets have the multi-direction and the detectors can not get the precise flow directions of the supplying air. Nevertheless, the maximum velocities in P5 and P6 collected by DDAS are very close to the CFD results, where there are only 1-4% gaps between them.

#### CONCLUSIONS

It can be concluded that irregularly distributed outlets on the bottom and inlets on the top can make the air flow direction turbulence in the chamber. The good design of the inlets and outlets may contribute to the better controlling velocity in the chamber so that the tobacco smoke can move in regular flow lines in the workplace. This can also decrease the turbulent circuit and reduce the dust deposit in the chamber. Moreover, the max velocity of diverse planes or lines are different form each other. Especially, the points with high air flow velocities closely to 1.00 m sec<sup>-1</sup> are located in the inlets and the outlets far away from them.

The CFD numerical modeling technique shown here in this study proves to be very useful in initiating

further and more comprehensive numerical study of the air flow distribution for the chamber with low pressure. The distance-data acquisition system used in the experimental test can prove validity of CFD results.

#### ACKNOWLEDGMENT

This study was supported by High School Funding Scheme for Key Young Teachers, Key Project of Henan Department of Science and Technology (102102210440).

#### REFERENCES

- Bauman, F.S. and E.A. Arens, 1988. The Development of a Controlled Environment Chamber for Physical and Subjective Assessment of Human Comfort in Office Buildings. In: A New Frontier: Environments for Innovation, Proceedings of the International Symposium on Advanced Comfort Systems for the Work Environment, May 1-3, 1988, Kroner, W.M. (Ed.). Center for Architectural Research, Troy, New York.
- CNIS GBZ1, 2010. Hygienic standard for the design of industrial enterprises. General Administration of Quality Supervision, Inspection and Quarantine of the People's Republic of China, China National Institute of Standardization, Beijing, China.
- Fish, W.J., D. Faulkner, D. Pih, P.J. McNeel, F.S. Bauman and E.A. Arens, 1991. Indoor air flow and pollutant removal in a room with task ventilation. Indoor Air, 3: 247-262.
- Panagopoulos, I.K., A.N. Karayannis, P. Kassomenos and K. Aravossis, 2011. A CFD simulation study of VOC and formaldehyde indoor air pollution dispersion in an apartment as part of an indoor pollution management plan. Aerosol Air Qual. Res., 11: 758-762.
- U.S. DHHS, 2006. The health consequences of involuntary exposure to tobacco smoke: A report of the Surgeon General. National Center for Chronic Disease Prevention and Health Promotion, Office on Smoking and Health, 93. U.S. Department of Health and Human Services, Centers for Disease Control and Prevention.
- WHO, 2008. WHO Report on the Global Tobacco Epidemic 2008: The MPOWER Package. World Health Organization, Geneva.